

# Direct Numerical Simulations of Fundamental Turbulent Flows with the Largest Grid Numbers in the World and its Application of Modeling for Engineering Turbulent Flows

Project Representative

Chuichi Arakawa Graduate School of Interdisciplinary Information Studies, the University of Tokyo

Authors

Chuichi Arakawa Graduate School of Interdisciplinary Information Studies, the University of Tokyo

Makoto Iida Graduate School of Engineering, the University of Tokyo

Yukio Kaneda Graduate School of Engineering, Nagoya University

Takashi Ishihara Graduate School of Engineering, Nagoya University

Hiroshi Kawamura Department of Mechanical Engineering, Tokyo University of Science

Tetsuro Tamura Interdisciplinary Graduate School of Science and Engineering, Tokyo Institute of Technology

In order to understand universal nature of turbulence, we performed large-scale direct numerical simulations (DNS's) of canonical incompressible turbulence on the Earth Simulator, including those of (i) turbulence in a periodic box and (ii) turbulent Ekman boundary layer. The DNS data were analyzed to study (i) the decay of isotropic turbulence and (ii) Reynolds number dependence and the three-dimensional characteristics in the turbulent Ekman boundary layer. Data analyses based on a wavelet-based method and those based on the multifractal model of turbulence were also made by using data obtained by the high-resolution DNS of forced incompressible turbulence in a periodic box.

We also performed numerical simulation of turbulent flows on the ES from the view point of engineering applications. We made a large eddy simulation for urban turbulent boundary layer. The information obtained by the LES will be utilized to solve the recent environmental problems such as air pollution and heat island in the urban area, also to establish the secure and safe society against the hazardous gasses at the center of city. We also made a detached eddy simulation (DES) for wake flow fields of a wind turbine. Aerodynamic performance and structure of wake flow behind a wind turbine were predicted for some wind speeds.

**Keywords:** High-resolution DNS, incompressible turbulence, turbulent Ekman boundary layer, database, urban turbulent boundary layer, DES, wind turbine, wake

## 1. High-resolution DNS's of incompressible turbulence in a periodic box

High-resolution direct numerical simulations (DNS's) of incompressible turbulence are effective in studying universal nature of turbulence because they provide us with detailed data of high-Reynolds-number turbulence free from experimental uncertainties. Here we present results obtained by a recent numerical experiment using the DNS of incompressible turbulence in a periodic box [1] and those obtained by recent data analyses based on the DNS of forced incompressible turbulence in a periodic box with the number of grid points up to  $2048^3$  on the Earth Simulator (ES) [2].

### 1.1 The decay of isotropic turbulence

In order to investigate the decay of freely evolving isotropic turbulence, direct numerical simulations of incom-

pressible turbulence were performed on the ES with the number of grid points up to  $1024^3$  [1]. There are two canonical cases in the decay of freely evolving turbulence. One is  $E(k \rightarrow 0) \sim Lk^2$  and the other is  $E(k \rightarrow 0) \sim Ik^4$ , where  $E(k)$  is the energy spectrum,  $k$  the wavenumber, and  $L$  and  $I$  the Saffman and Loitsyansky integrals respectively. We focused on the second of these. The DNS's were performed in a periodic domain whose dimensions,  $l_{box}$ , are much larger than the integral scale of the turbulence,  $l$ . It found that, provided that  $l_{box}/l$  and the Reynolds number are much larger than unity,  $I$  tends to an (almost) constant value and Kolmogorov's classical decay law,  $u^2 \sim t^{-10/7}$ , holds true as the turbulence matures. The approximate conservation of  $I$  in fully developed turbulence implies that the long-range interactions, as measured by the triple correlations, are very weak.

### 1.2 Data analysis based on a wavelet-based method

A wavelet-based method to extract coherent vortices is applied to data obtained by DNS of three-dimensional homogeneous isotropic turbulence performed for different Taylor microscale Reynolds numbers, ranging from  $R_\lambda=167$  to 732, in order to study their role with respect to the flow intermittency.

As the Reynolds number increases, the percentage of wavelet coefficients representing the coherent vortices decreases, i.e. flow intermittency increases. Although the number of degrees of freedom necessary to track the coherent vortices remains small, they preserve the nonlinear dynamics of the flow [3]. We observe a strong scale-by-scale correlation between the velocity field induced by the vortices and the total velocity field over the scales retained by the data [4]. It is thus conjectured that the wavelet representation could significantly reduce the number of degrees of freedom to compute fully-developed turbulent flows as the Reynolds number increases.

### 1.3 Data analysis based on the multifractal model of turbulence

Several intermittent fields coexist in a high-Reynolds-number turbulence. To characterize the mutual relation between intermittencies associated with the measures  $\varepsilon$  (rate of energy dissipation) and  $\Omega$  (enstrophy), a multifractal analysis based on  $\varepsilon$  and  $\Omega$  in isotropic turbulence is made by using high-resolution direct numerical simulation of turbulence with the number of grid points up to  $2048^3$ [5]. The analysis shows that the singularity exponents  $\alpha$  and  $\alpha'$  that characterize the intermittencies associated with  $\varepsilon$  and  $\Omega$ , respectively, agree well with each other in the inertial subrange, and also that the correlation coefficient  $\rho$  between  $\alpha$  and  $\alpha'$  is approximately 1.0 in the inertial subrange. These results are consistent with  $\log \varepsilon_r$  and  $\log \Omega_r$  correlating well with each other for the scale  $r$  in the inertial subrange, where the subscript denotes the local average over a cubic domain of size  $r$ . Note that the correlation coefficient  $\rho$  between  $\alpha$  for  $(\partial u_i/\partial t)^2$  and  $\alpha'$  for  $\omega_x^2$  obtained from atmospheric data at high Reynolds number was approximately 0.3[6]. The difference between  $\rho \sim 0.3$  for  $(\partial u_i/\partial t)^2$  and  $\omega_x^2$  and  $\rho \sim 1.0$  for  $\varepsilon$  and  $\Omega$  presents an example that the statistics obtained experimentally, using the one-dimensional surrogates, are different from the original ones.

## 2. DNS's of turbulent Ekman boundary layer

Rotation is one of the factors which affect the planetary boundary layer. The boundary layer under the effect of the system rotation is called the Ekman boundary layer. (EBL) The Ekman boundary layer is three-dimensional flow in nature, in which three forces are balanced, i.e., the pressure gradient, viscous and the Coriolis forces.

In the present study, we calculated DNSs of the neutrally

stratified turbulent Ekman boundary layer up to the Reynolds numbers of  $Re_f = 1393$  where  $Re_f$  is based on the geostrophic wind, the kinematic viscosity and Coriolis parameter. Our objective is to investigate Reynolds number dependence and the three-dimensional characteristics in the turbulent Ekman boundary layer, and to obtain its DNS database.

Fig. 1 shows the database site on the turbulent Ekman layer at Tokyo University of Science [7]. Turbulence statistics such as the profiles of the mean velocity, the Reynolds stresses and the budgets of the Reynolds stresses are presented. The number of access for the database is about 2000 per year so that it would contribute to develop a more accurate turbulence model.

A paper about the three-dimensional characteristics of the turbulence structures is published in Journal of the Earth Simulator [8]. For instance, a motion of a passive material line in EBL is visualized in Fig. 2. The material line is initially released from a vicinity of the wall ( $y^+ = 17$ ). Figure 2 shows the state of the material line at  $t^+ = 162$  after the release. A strong ejection event is observed in the oval A in Fig. 2. If the advected spanwise distance is compared for the

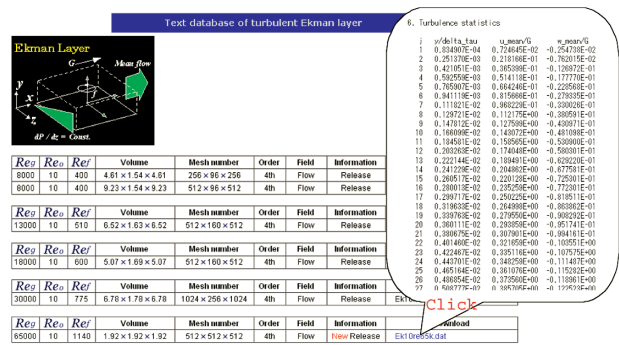


Fig. 1 Database site on the turbulent Ekman layer at Tokyo University of Science [7].

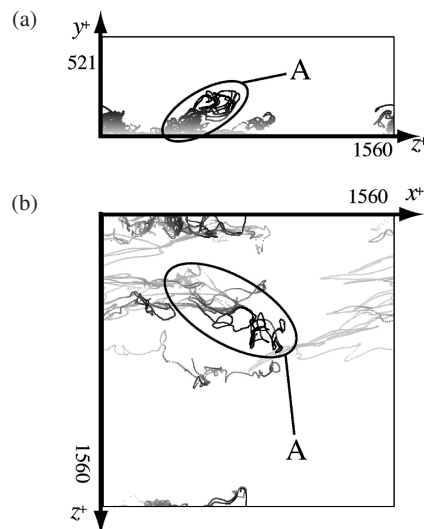


Fig. 2 A motion of a material line after  $t^+ = 162$  for  $Re_f = 400$ . The color indicates the height from the bottom wall, gray to black,  $y^+ = 0$  to  $y^+ = 182$ . (a) Side view from left side of (b), (b) top view.

material line raised up to the outer region and the one staying in the vicinity of the wall, the distance of the former one is smaller than that of the latter. This is because the spanwise mean velocity is larger in the vicinity of the wall than in the outer region. In fact, the spanwise movement of the material line near the wall in the oval A is roughly equal to the product of the mean spanwise velocity and the elapsed time. Therefore, the inclination of the large-scale structure is caused by the combination of the strong ejection and the three-dimensional mean velocity profile.

### 3. Large eddy simulation for urban turbulent boundary layer

Large eddy simulation for urban turbulent boundary layer has been carried out. In order to construct an urban numerical model, we introduce various shapes of rectangular blocks and distribute them on a flat plate. For the spatially developing type of boundary layers, the quasi-periodic boundary method using the re-scaling concept was applied to the inlet boundary conditions. Details of unsteady flows in the near wall region were examined, especially focusing on the coherent structures of atmosphere-like turbulence over the roughness blocks as well as fine structures of canopy flows near the ground surface (a typical turbulence structures over and within the forest canopy can be seen in Fig. 3). The computed turbulence statistics were compared with the previous experimental data and the numerical accuracy has been confirmed. Various physical parameters such as roughness length and zero displacement were estimated for very rough-wall turbulent boundary layers. New similarity concept for turbulent boundary layer over urban-like very large-scaled roughness was introduced and fully discussed. The

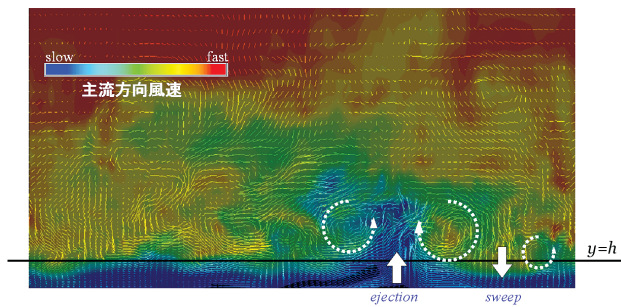


Fig. 3 Instantaneous turbulence structures over and within the forest canopy.

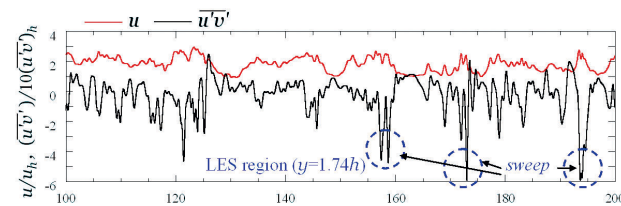


Fig. 4 Time variations of streamwise velocity and Reynolds shear stress above the vegetation.

information obtained by LES will be utilized to solve the recent environmental problems such as air pollution and heat island in the urban area, also to establish the secure and safe society against the hazardous gasses at the center of city.

We also have carried out LES for the turbulent boundary layer over the forest and turbulence structures over and within the vegetation canopy are investigated. Figure 4 shows the time variations of streamwise velocity and Reynolds shear stress above the vegetation. The information concerning the flows in forest was provided for estimating the  $\text{CO}_2$  absorption or the airborne pollen among trees.

### 4. Detached eddy simulation (DES) for wake flow fields of a wind turbine

Wake flow fields of a wind turbine have not been less well understood because there are very complex structures of turbulent flow fields around a wind turbine blade. In order to elucidate structure of wake and construct a numerical wake model, the flow field is calculated with a Detached-Eddy-Simulation (DES) in this study. DES is a method for predicting turbulence in computational fluid dynamic simulations by coupling RANS methods for the boundary layer and LES for the free shear flow. The object of this simulation is the flow around rotating NREL Phase VI wind turbine blade. Simulation results are compared with experimental data by NREL. The simulated wind turbine is upwind type with two blades which has a diameter of about 10 m and operates at wind speeds of 7 m/s, 10m/s, 20m/s. As setting a computational domain, it was important to consider extent of computational domain and its fineness because effects of wake is propagated far away from the rotor blade and the resolution of wake is strongly affected by fineness of computational domain especially in downstream of the rotor. A single block grid is used in present study. Since the wind turbine has 2 blades in this case, the domain is chosen to consist of half a sphere. Only one of the blades is explicitly modeled in the simulation. The remaining blade is accounted for using periodic boundary conditions, exploiting the 180 degrees symmetry of the two-bladed rotor. Uniform flow,  $U$ , corresponding to the wind speed is prescribed in the x-direction. The blade rotates about the x-axis. The outer boundary of the computational domain is located 2 rotor radii away from the center of rotation. The Grid is consisting of 301 grid points along the airfoil surface ( $\xi$ -direction), 130 grid points perpendicular to the airfoil surface ( $\eta$ -direction), and 257 grid points along the span direction ( $\zeta$ -direction). The total number of grid points is about 10 million.  $\Delta y^+$  is set to take a value of approximately 1.0 along the entire blade surface. No wall model is used. As one of the simulation results in the vicinity of the blade, Fig. 5 shows the pressure coefficient at each span-wise position for  $U = 10.0$  m/s ( $\lambda = 3.8$ ). The result of 2.3million grid points illustrates in the same

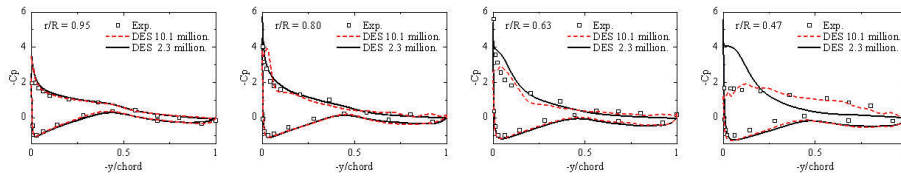
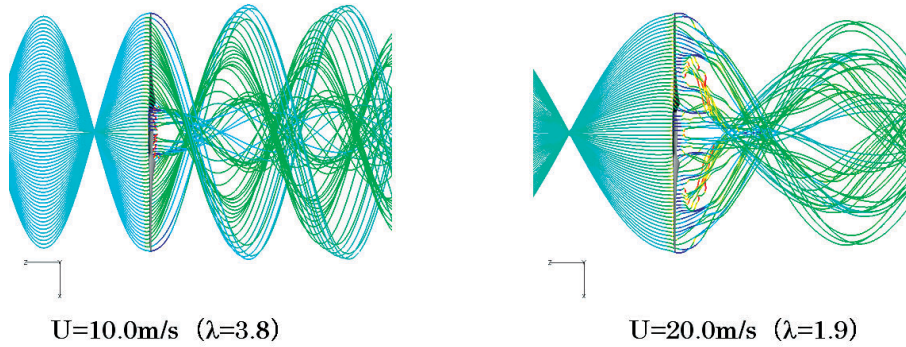
Fig. 5 Pressure coefficient for  $U = 10.0$  m/s.

Fig. 6 Streamline and stream-wise velocity contours.

figure. 10 million grid points is good agreement with experimental data. The streamlines and stream-wise velocity contours for  $U = 10.0$  m/s and  $U = 20.0$  m/s cause in wake flow of the wind turbine can be seen in Fig. 6. There are completely different in two cases. There are very complex structures behind the blade. Especially for  $U = 20.0$  m/s, figure shows that the strongly vortex structure is borne on the flow.

## 5. Summary

Several basic researches are carried out in direct numerical simulations for turbulent flows where new information are derived and will contribute to the turbulent modeling for applications. Additionally, the application for wind turbines is found to be available for developing new trend of machines in the frame of giant simulation with the Earth Simulator.

## References

- [1] T. Ishida, P.A. Davidson and Y. Kaneda: "On the decay of isotropic turbulence," *J. Fluid Mech.* vol.564, pp.455–475, 2006.
- [2] Y. Kaneda, T. Ishihara, M. Yokokawa, K. Itakura and A. Uno: "Energy dissipation rate and energy spectrum in high resolution direct numerical simulations of turbulence in a periodic box," *Phys. Fluids*, vol.15, no.2, pp.L21–L24, 2003.
- [3] N. Okamoto, K. Yoshimatsu, K. Schneider, M. Farge, and Y. Kaneda: "Coherent vortices in high resolution DNS of homo geneous isotropic turbulence : a wavelet viewpoint," 2007. (*submitted*)
- [4] K. Yoshimatsu, N. Okamoto, K. Schneider, M. Farge, and Y. Kaneda: "Wavelet-based extraction of coherent vortices from high Reynolds number homogeneous isotropic turbulence," *IUTAM Symposium on Computational Physics and New Perspectives in Turbulence*, Nagoya, 2006, ed by Y. Kaneda, Springer-Verlag, (*accepted*)
- [5] T. Ishihara and H. Higuchi: "Multifractal Analysis by Using High-Resolution Direct Numerical Simulation of Turbulence," *IUTAM Symposium on Computational Physics and New Perspectives in Turbulence*, 2006, Nagoya, ed by Y. Kaneda, Springer-Verlag, (*accepted*)
- [6] C. Meneveau, K. R. Sreenivasan, R. Kailasnath, and M.S. Fan: "Joint multifractal measures: Theory and applications to turbulence" *Phys. Rev. A*, vol.41, pp.894–913 (1990)
- [7] <http://murasun.me.noda.tus.ac.jp/>
- [8] K. Miyashita, K. Iwamoto and H. Kawamura: "Direct Numerical Simulation of the Neutrally Stratified Turbulent Ekman Boundary Layer," *Journal of the Earth Simulator*, **6**, (2006), 3–15.

# 乱流の世界最大規模直接計算とモデリングによる応用計算

プロジェクト責任者

荒川 忠一 東京大学 大学院情報学環

著者

荒川 忠一 東京大学 大学院情報学環

飯田 誠 東京大学 大学院工学研究科

金田 行雄 名古屋大学 大学院工学研究科

河村 洋 東京理科大学 理工学部 機械工学科

田村 哲郎 東京工業大学 大学院総合理工学研究科

石原 卓 名古屋大学 大学院工学研究科

乱流の普遍的な性質を理解するため、我々は規範的(カノニカル)な非圧縮性乱流の大規模直接数値計算(DNS)を行った。ひとつは(i)周期境界条件における一様等方性乱流であり、もうひとつは(ii)回転を伴う乱流境界層(エクマン境界層)である。得られた乱流データは各々、(i)等方性乱流における減衰法則を調べるため、(ii)エクマン境界層における乱流統計量とそのレイノルズ数依存性を調べるために解析した。また、ウェーブレット変換を基にしたデータ解析や乱流のマルチフラクタルモデルを基にしたデータ解析も一様等方性乱流の世界最大規模DNSデータを用いて行った。なお、(ii)で得られた乱流のDNSデータはこれまでに行われたエクマン境界層のDNSにおいて最大のレイノルズ数を実現したものであり、その解析により得られた乱流統計量等は、現在、東京理科大学のWebサイトで公開中である。

応用研究としては都市境界層のLES大規模計算を行った。種々のブロックで構成される擬似的な都市モデルを対象に、大気乱流のブロック上方での大規模構造から地表面近傍の微細構造まで明らかにすることで、近年の大気汚染、ヒートアイランド現象の環境問題を解決し、あるいは都市の人が大勢集まる場所での危険物質の拡散事故などに対して、安全で安心な街を創出する指針を示すべく、都市に形成される風環境の特異性について明らかにした。また、森林などの植生上を発達する乱流境界層に関して、LESとRANSのハイブリッド計算を実施し、植生キャノピー内外の乱流現象を明らかにし、森林でのCO<sub>2</sub>吸収あるいは花粉放出の状況を判断するための流れ特性に関する情報を提示した。

また、風車後流の大規模計算を行った。風車後流の流れ構造は、未だ解明されていない。それは、風車翼周りでは層流・乱流境界層、翼端渦などの異なるスケールの乱流構造が存在し、加えて自然風の影響による変動も影響し、多くの要因が関係するからである。本研究では、DESを用いた風車後流解析を行い、流入風の影響を調べた。

キーワード：大規模直接数値計算, 非圧縮性乱流, エクマン境界層, 都市境界層